Anatomical image-based rigid registration between fluoroscopic X-ray and CT: methods comparison and experimental results

L. Joskowicz[1],D. Knaan[1],H. Livyatan[1],Z. Yaniv[1],A. Khoury[2],R. Mosheiff[2],M. Liebergall[2]

[1] School of Computer Science and Eng., The Hebrew Univ. of Jerusalem, Israel
[2] Orthopaedic Surgery Dept., The Hadassah-Hebrew Univ. Medical School, Israel.
E-mail: josko@cs.huji.ac.il, WWW site: http://www.cs.huji.ac.il/~josko

This paper describes a practical, whole system approach to rigid registration between preoperative CT and intraoperative X-rays obtained with a tracked C-arm and demonstrates its efficacy experimentally. Our approach is generic, targeted to orthopaedic surgery and includes fluoroscopic X-ray calibration, image distortion correction, optical tracking, and 2D/3D image registration. For 2D/3D image registration, we use two new gradient-based and intensity-based algorithms which are fast, robust, and accurate in realistic setups. Our experiments on simulated, in-vitro, and cadaver show that an overall mean target registration error of 1–1.5mm (2mm worst case), which succeeds on the first try 95% or more of the time in less than two minutes, is practically feasible.

1. INTRODUCTION

Registration is an essential step in most Computer-Aided Surgery systems (CAS). It consists of finding a transformation that aligns common features from two modality data sets taken at different times [1]. It is required in image-guided and robotic surgery to match preoperative images and plans to the intraoperative situation, to determine the relative position of surgical tools and anatomy, and to position a robot and monitor its motion relative to the anatomy. A few dozen CAS systems have been developed over the past ten years, mainly for neurosurgery and for orthopaedic surgery [2].

Practical, accurate, and robust registration is one of the key technical challenges of CAS. Current systems rely on implanted fiducials, which require additional surgery, or on points harvested on the surface anatomy by direct contact, which requires usually additional anatomical exposure. Instead, bone shapes in intraoperative fluoroscopic X-ray images, which are rigid, can be used. Anatomical image-based registration is non-invasive, is potentially faster, and is less prone to human error. However, it is technically much harder because it requires analyzing the fluoroscopic X-ray images, which have a small field of view, have limited resolution, have orientation-dependent geometric and intensity distortions, and may contain surgical tools and implants not present in the CT.

Due to its great potential, many researchers developed algorithms for X-ray to CT 2D/3D rigid registration. Geometry-based algorithms match selected geometric features from each data set by finding the transformation that minimizes the sum of distances between paired features [4–6]. Intensity-based algorithms match the intensities of one

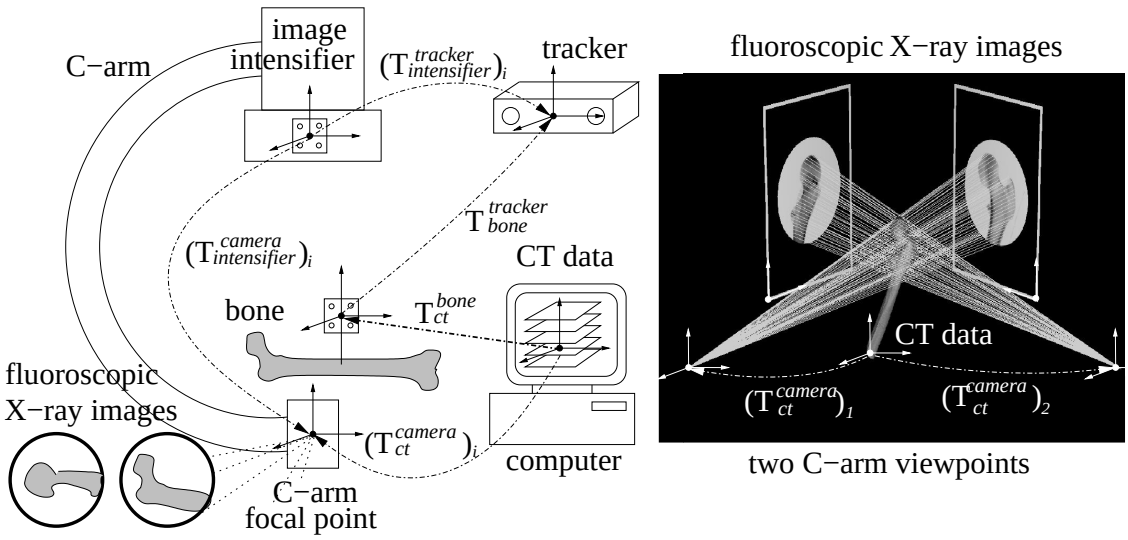

Figure 1. Registration chain between the actual bone and its preoperative CT (left) and 2D/3D image registration geometry between X-ray and CT (right).

image data set with the intensity of the other by minimizing a measure of difference between them [7–10]. However, with the exception of the Cyberknife system [3], none of them is in routine clinical use. The main obstacles are robustness, accuracy, efficiency, and system integration.

2. MATERIALS AND METHODS

We have developed a practical, fast, and robust whole system approach to anatomical image-based rigid registration between preoperative CT images and intraoperative fluoroscopic X-ray images. The approach is generic, customizable, and is targeted for routine clinical use in orthopaedic surgery. It is non-invasive, anatomy-based, requires minimal user training and interaction, and includes validation. Following an in-depth analysis of the most common orthopaedic procedures, we set our goal to obtain a registration with an overall mean surface target registration error (sTRE) of 1–1.5mm (2mm worst case) on the first try at least 95% of the time in less than two minutes on a CT data set with 1mm thick slices 1.5mm apart and 2–5 fluoroscopic X-ray images from different viewpoints, possibly with foreign objects, and C-arm localization of 0.3–0.5mm.

To compute the rigid transformation T^{bone}_{ct} that relates the preoperative CT data to the intraoperative X-ray images, we use a location tracker and a fluoroscopic X-ray C-arm (Fig. 1). The registration chain consists of five transformations:

$$(T^{camera}_{ct})_i = (T^{camera}_{intensifier})_i \cdot (T^{tracker}_{intensifier})^{-1}_i \cdot T^{tracker}_{bone} \cdot T^{bone}_{ct}$$

where i indicates the C-arm viewpoint. $(T^{tracker}_{intensifier})_i$ and $T^{tracker}_{bone}$ are given directly by the tracker. The calibration transformations $(T^{camera}_{intensifier})_i$ is computed as described in [11]. The transformations $(T^{camera}_{ct})_i$ are computed from the initial pose estimate T^{bone}_{ct} with a 2D/3D rigid registration algorithm, which successively refines them until convergence.

For 2D/3D rigid registration we use a gradient-based [12] and an intensity-based algorithm [13]. Both require an initial bone pose estimation, which can be determined from the clinical setup, estimated from skin markers, or computed from a few surgeon-defined matching landmarks on the CT and fluoroscopic X-ray images.

The gradient-based algorithm [12] consists of coarse geometry-based registration followed by fine Gradient Projection Registration (GPR) on edge pixels. Coarse registration reduces the distance between the bone surface mesh and sampled points on the fluoroscopic X-ray bone contours with the Iterative Closest Point method [4]. It yields the best transformation that can be obtained from the segmented images, which may have occlusions and include foreign objects. GPR further reduces the difference by incorporating contour pixel and volume gradient data. It eliminates foreign objects which appear in the X-ray images and not in the CT data, and does not rely on the segmentation accuracy.

The intensity registration algorithm [13] consists of 1. generation of Digitally Reconstructed Radiographs (DRRs) for each viewpoint; 2. pose difference measurement by comparing the DRRs with the real fluoroscopic X-ray images, and 3. computation of C-arm viewpoints that minimize the difference. It improves upon existing methods and overcomes the speed, robustness, and accuracy problems intrinsic to intensity-based registration. To speed up DRR generation. we compute them only in ROIs dynamically selected on the fluoroscopic X-ray images based on pixel gray value variance. In addition, we use a pyramid of downsampled fluoroscopic X-ray images, and precompute the gray levels of rays in all viewing directions in a Transgraph data structure [10]. We use a fast non-gradient downhill simplex optimization to search for the C-arm viewpoint. For robustness, we use a genetic algorithm to reduce the likelihood of local minima convergence. To widen the initial pose range, we first apply the Normalized Cross Correlation comparison measure and then the Variance Weighted Sum of Local Normalized Correlation [10]. The latter measure yields high accuracy because it emphasizes areas with more variance.

3. EXPERIMENTAL RESULTS

We implemented the entire registration process with both the gradient and intensity-based 2D/3D rigid algorithms, and validated it in three situations: 1. simulation experiments with clinical CT data and simulated fluoroscopic X-rays; 2. in-vitro experiments with dry bones, and; 3. a cadaver experiment. The simulation experiments establish the registration algorithms accuracy with no fluoroscopic X-ray imaging and tracking errors. The in-vitro experiments establish the overall error for real CT, fluoroscopic X-ray images, and tracking under ideal conditions. The cadaver experiment emulates the surgical situation and establishes the expected navigation error. We demonstrate the genericity of our method by applying it to four anatomical structures: human femur, spine, pelvis, and lamb hip. Fig. 2 and Tab. 1 summarize the results.

We used a CT scanner (Marconi, USA), a 9" BV29 C-arm (Phillips, The Netherlands), a Polaris optical tracking camera (NDI, Canada), a FluoroTrax C-arm calibration ring and active optical trackers (Traxtal, Canada), and a Matrox Meteor II digital frame grabber. Processing was on a 2.4Ghz, 1GB RAM PC under Windows XP. All CT scans were at 0.6mm slice interval and 0.5mm slice thickness except for the pelvis CT.

We performed a simulation experiment on a clinical pelvis CT. We generated DRRs at

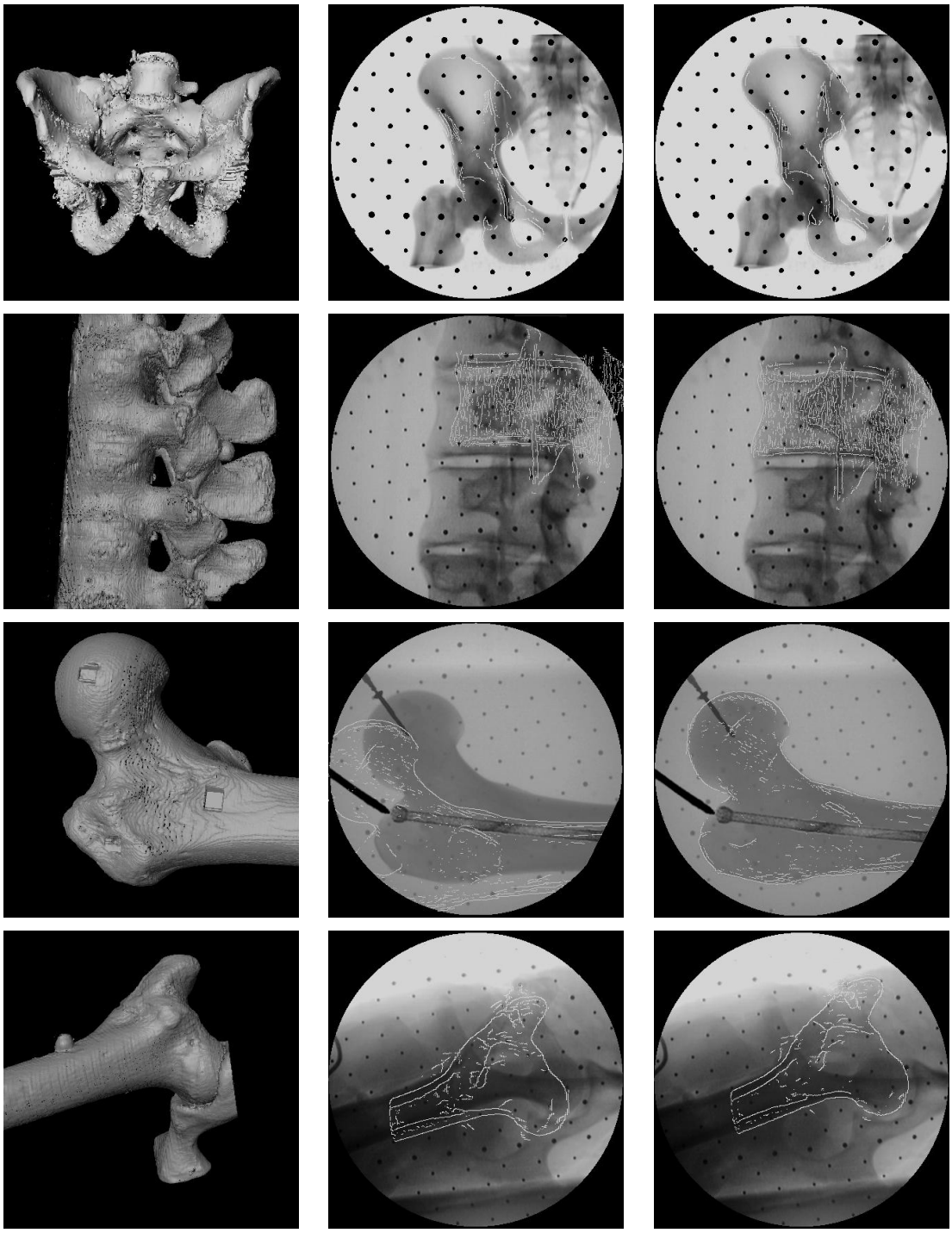

(a) CT model (b) before registration (c) after registration

Figure 2. Registration results: real pelvis with simulated fluoroscopic X-ray images (DRRs), in-vitro dry spine and dry femur with surgical instruments, and cadaver lamb hip. The first column shows the CT model. The second and third column show one fluoroscopic X-ray image with contours at initial and final pose superimposed on them (white lines). The gradient and intensity-based results are visually identical.

Data set	Ideal $\Delta h = 0.6$mm, none		Realistic $\Delta h = 2.4$mm, some		Worst-case $\Delta h = 4.2$mm, some	
SIMULATION						
1. real pelvis	———		0.5 (0.8)	0.3 (0.7)	0.6 (0.8)	0.5 (0.7)
IN VITRO						
3. dry spine	0.4 (0.5)	0.3 (0.4)	0.5 (0.6)	0.4 (0.7)	0.6 (1.0)	0.7 (1.5)
2. dry femur	0.6 (0.8)	0.7 (1.1)	1.1 (1.5)	0.9 (1.8)	1.3 (1.6)	1.6 (3.4)
CADAVER						
4. lamb hip	1.2 (1.6)	1.0 (1.1)	1.4 (2.5)	1.1 (1.8)	1.7 (3.0)	1.3 (2.4)

Table 1
Summary of experimental results. Each entry shows the mean (maximum) surface target registration error (sTRE) in millimeters for gradient-based (left) and intensity-based (right) registration. Each scenario (ideal, realistic, and worst-case) is defined by the CT slice spacing Δh and the presence of foreign objects in the fluoroscopic X-ray images. Three fluoroscopic X-ray images were used in all cases except the pelvis, where five images were used. Computation times are 20–100 secs.

known camera viewpoints to simulate fluoroscopic X-ray images. We offset each viewpoint point by about 10m, which is a large initial guess sTRE. The mean sTRE for both methods is 0.5mm, which is about size of X-ray image pixel. This is probably the best possible result obtainable with a CT data set with 2.4mm slice interval and 1.5mm slice thickness because of the low DRR quality.

We performed in-vitro experiments on a single vertebra of a dry spine and on a dry proximal femur. First, we implanted seven 6mm aluminum spheres and CT scanned them. We extracted the sphere centers to a mean accuracy of 0.1mm (0.3mm max). We then acquired two sets of three fluoroscopic X-ray images at various C-arm viewpoints, one with, and one without anatomy for optimal C-arm calibration. We performed C-arm calibration to mean accuracy of 0.3mm (0.6mm max), and obtained a ground-truth registration by fiducial contact-based registration on the spheres to an accuracy of 0.3mm (0.5mm max). We then performed 2D/3D registration and compared the resulting transformations. We obtained an average sTRE of 1mm, and 99% (90%) success with 25–40mm (45–60mm) offset for the femur, 0–10mm (10–25mm) for the vertebra. The error increased for two fluoroscopic X-ray images, but did not decrease for three or more. There was a small decrease in accuracy when some foreign objects were present.

We performed a cadaver experiment on a fresh lamb hip with the same in-vitro protocol, except that we used only four fiducials. The decreased accuracy, which is still clinically acceptable, was due to a less accurate ground-truth registration and to the fact that the lamb femur has fewer salient features than the other anatomical structures.

We found that the gradient and intensity-based 2D/3D registration algorithms are comparable in terms of accuracy, with the latter having a smaller sTRE standard deviation. The intensity-based method proved to be more robust (less failures) and have a larger convergence range interval because it uses a genetic algorithm and two comparison measures. However, it depends on coarse initial viewpoint estimations to generate the Transgraph.

4. CONCLUSION

We conclude from our experimental results that anatomical image-based rigid registration between preoperative X-ray and intraoperative CT with an overall mean surface target registration error of 1–1.5mm (2mm worst case), which succeeds on the first try 95% or more of the time in less than two minutes, is practically feasible. The most sensitive step of the registration chain is the C-arm calibration. Gradient and intensity-based 2D/3D rigid registration methods are comparable, and they are superior to geometry-based registration because they use more CT information and do not rely on high-quality image segmentation.

ACKNOWLEDMENT:
This research was supported in part by a grant from the Israel Ministry of Industry and Trade for the IZMEL Consortium on Image-Guided Therapy.

REFERENCES

1. Maintz, J.B.A. and Viergever, M.A., A survey of medical image registration, *Medical Image Analysis* 2(1), 1998.
2. Nolte, L. P. and Ganz, R., *Computer Assisted Orthopedic Surgery*, Hogrefe&Huber Publishers, 1999.
3. Adler J. Jr., Murphy, M., Chang, S. and Hancock, S., Image-guided robotic radiosurgery, *Neurosurgery* 44(6), 1999.
4. Besl, P. and McKay, N. A method for registration of 3D shapes, *IEEE Trans. on Pattern Analysis and Machine Intelligence* 14(2), 1992.
5. Hamadeh, A., Lavallée, S. and Cinquin, P., 'Automated 3-dimensional computed tomographic and fluoroscopic image registration, *Computer Aided Surgery* 3(1), 1998.
6. Guéziec, A., Kazanzides, P., Williamson, B., and Taylor, R.H., Anatomy based registration of CT-scan and intraoperative X-ray images for guiding a surgical robot, *IEEE Transactions on Medical Imaging* 17(5), 1998.
7. Lemieux, L., Jagoe, R., Fish, R. *et al.*, A patient-to-computed-tomography image registration method based on DRRs, *Medical Physics* 21(11), 1994.
8. Murphy, M.J., An automatic six-degree-of-freedom registration algorithm for image-guided frameless stereotactic radiosurgery, *Medical Physics* 24(6), 1997.
9. Roth, M., Brack, C., Burgkart, R., and Czopf, A., Multi-view contourless registration of bone structures using a single calibrated x-ray fluoroscope, *Proc. of the Computer-Assisted Radiology and Surgery Conf.*, 1999.
10. LaRose, D.A, Bayouth, J., and Kanade, T., Transgraph: interactive intensity-based 2D/3D registration of X-ray and CT data, in *SPIE Image Processing*, 2000.
11. Livyatan, H., Yaniv, Z., and Joskowicz, L. Robust automatic C-arm calibration for fluoroscopy-based navigation: a practical approach, *Proc 5th Int. Conf. on Medical Image Computing and Computer-Aided Intervention*, Tokyo, Japan, 2002.
12. Livyatan, H. *Gradient-based 2D/3D rigid registration of fluoroscopic X-ray to CT*, MSc. Thesis, The Hebrew University of Jerusalem, Israel, June 2003.
13. Knaan, D. *Intensity-based 2D/3D rigid registration of fluoroscopic X-ray to CT*, MSc. Thesis, The Hebrew University of Jerusalem, Israel, June 2003.